



## Biodegradable Polymeric Nanoparticles for Photodynamic Laser Cancer Therapy

**Mohammadreza Saboktakin\***

Professor, Nanomedicine Department, NanoBMat Company GmbH, Düsseldorf, Germany

\*Corresponding Author: Mohammadreza Saboktakin, Professor, Nanomedicine Department, NanoBMat Company GmbH, Düsseldorf, Germany.

**Received:** April 08, 2021

**Published:** May 11, 2021

© All rights are reserved by **Mohammadreza Saboktakin.**

### Abstract

Photodynamic cancer therapy is well known and recognized in many countries best therapy for cancer therapy. However, previous findings on PDT are limited to Tumors on the body surface, since the available photosensitizers largely from Porphyrin exist and can only be stimulated with red laser light. The penetration depth of the red laser with effective stimulation of the photosensitizer is about 1 - 2 cm and also limited to a tumor size of about 1 cm. The penetration into the liver or through bone is almost impossible, so that there is no possibility. To successfully treat liver metastases or brain tumors. Infrared laser beams penetrate a lot deeper into the body and can even penetrate liver and bone. A perfect one Photosensitizer should therefore have an absorption spectrum in the infrared range, in the market however, nothing is available. The new polymeric systems have reviewed in this review.

**Keywords:** Liver; Bone; Cancer Therapy; Nanoparticles

*In vitro* photocytotoxicity and cellular uptake of biodegradable polymeric nanoparticles loaded with photosensitizer mTHPP have been studied. As the first part of a continued research on conversion of N-sulfonato-N, Ocarboxymethylchitosan (NOCCS) to useful biopolymer-based materials, large numbers of carboxylic functional groups were introduced onto NOCCS by grafting with polymethacrylic acid (PMAA). The free radical graft copolymerization was carried out at 70 °C, bis-acrylamide as a cross-linking agent and persulfate as an initiator. These results show that the nanoparticles have high loading capacity and stability. These nanoparticles are suitable as carriers for photodynamic therapy *in vivo* [1]. mTHPP loaded NOCCS/PMAA nanoparticles by the classical method, which involves spreading a uniform layer of polymer dispersion followed by a drying step for removal of solvent system. Since the methodology of nanoparticles preparation involved a heating step, it may have had a detrimental effect on the chemical stability of drug. Hence, the stability assessment of mTHPP impregnated in nanoparticle was done using stability-indicating method. For this purpose,

mTHPP was extracted from polymer and analyzed by HPLC. A single peak at 14.8 minutes representing mTHPP (with no additional peaks) was detected in the chromatogram, suggesting that the molecule was stable during preparation of nanoparticles. The composition of the polymer defines its nature as a neutral or ionic network and furthermore, its hydrophilic/hydrophobic characteristics. Ionic hydrogels, which could be cationic, containing basic functional groups or anionic, containing acidic functional groups, have been reported to be very sensitive to changes in the environmental pH. Hydrogels containing basic functional groups is found increased swelling activity in acidic conditions and reduced in basic conditions. The pH sensitive anionic hydrogels shows low swelling activity in acidic medium and very high activity in basic medium. As observed from SEM photomicrographs, the crystals of mTHPP have a different appearance than recrystallized mTHPP. These nanoparticles do not have clearly defined crystal morphological features in the SEM photomicrographs. Hence, it appears that the irregularly shaped particle are surface deposited with poloxamer, which gives

them an appearance resembling that of coated particles. The thermal behavior of a polymer is important for controlling the release rate in order to have a suitable drug dosage form. The glass transition temperature ( $T_g$ ) was determined from the DSC thermograms. The higher  $T_g$  values probably related to the introduction of cross-links, which would decrease the flexibility of the chains and the ability of the chains to undergo segmental motion, which would increase the  $T_g$  values. On the other hand, the introduction of a strongly polar carboxylic acid group can increase the  $T_g$  value because of the formation of internal hydrogen bonds between the polymer chains. X-ray diffraction is a proven tool to study crystal lattice arrangements and it yields very useful information on degree of crystallinity. X-ray diffraction technique is also used to study the degree of crystallinity of pharmaceutical drugs and excipients. A lower  $2\theta$  value indicates larger spacings, while an increase in the number of high-angle reflections indicates higher molecular state order. In addition, broadness of reflections, high noise, and low peak intensities are characteristic of a poorly crystalline material. A broad hump in the diffraction pattern of chitosan extending over a large range of  $2\theta$  suggests that modified chitosan is present in amorphous state in the nanoparticles. It was shown that mTHPP/polymer feed ratios up to 30% (w/w), the loading efficiency was almost quantitative, resulting in loading capacities up to 30% and an mTHPP concentration in the dispersion of 1.8 mg/mL, which is markedly higher than the aqueous solubility of mTHPP. At 10% (w/w) loading, the dispersions stayed clear for more than a week. At higher loading of 20% and 30% (w/w), a precipitate was observed in the dispersions of loaded NOCCS/PMAA within 1 day after preparation, indicating that the loading capacity of these nanoparticles was exceeded. In contrast, the nanoparticles composed of polymer remained clear for more than a week at 20% and 2 days for 30% loading, which demonstrates that these end groups have a favorable effect on the loading and solubilization capacity of the nanoparticles. The *in vitro* photocytotoxicity effect of mTHPP loaded NOCCS/PMAA nanoparticles on 14C cells was determined after 6 h incubation and compared with free mTHPP. Either various dilutions of loaded nanoparticles at a fixed mTHPP/polymer ratio of 15% (w/w) were used, or the polymer concentration was fixed at 0.5 mg/mL and the mTHPP loading was varied between 0.004% and 0.32% (w/w) in order to secure a polymer concentration of ~100 times above its critical aggregation concentration. At a fixed high polymer concentration, the nanoparticles with various loadings were hardly toxic to cells even at the highest mTHPP concen-

tration used, as indicated by a cell viability of 80%. Loaded nanoparticles, and free mTHPP were diluted in medium to a concentration of 12  $\mu$ M mTHPP and incubated with 14C cells for 6 h to determine the cellular uptake of mTHPP. The 15% (w/w) mTHPP loaded and polymer nanoparticles showed a lower cellular uptake of mTHPP compared to free mTHPP, by a factor of 2.8 and 3.7, respectively. More importantly, hardly any mTHPP uptake was measured after incubation with the nanoparticles yielding a cellular uptake comparable of free mTHPP. The results of the photocytotoxicity and cellular uptake of the different formulations suggest that when the concentration of polymer is kept well above, mTHPP remains stably encapsulated in the nanoparticles even in the presence of serum, and that the intact nanoparticles are not taken up by the cells, which may be ascribed to the presence of a dense polymer-layer. Only after dilution of the mTHPP-loaded NOCCS/PMAA nanoparticles to polymer concentrations below and after nanoparticle degradation, the released mTHPP can be taken up by 14C cells and exert its cytotoxic effect upon illumination. Nano polymer bonded mTHPP (50 mg) were poured into 3 mL of aqueous buffer solution (pH 7.4). The mixture was introduced into a cellophane membrane dialysis bag. The bag was closed and transferred to a flask containing 20 mL of the same solution maintained at 37°C. The external solution was continuously stirred, and 3 mL samples were removed at selected intervals. The triplicate samples were analyzed by UV spectrophotometer, and the quantity of mTHPP were determined using a standard calibration curve obtained under the same conditions. The primary mechanism for release of mTHPP from matrix systems *in vitro* are swelling, diffusion, and disintegration. *In vitro* degradation of chitosan beads were prepared by solution casing method occurred less rapidly as the degree 73% deacetylated showed slower biodegradation. Since the grade of chitosan used in the present study was of high molecular weight with a degree of deacetylation  $\geq 85\%$ , significant retardation of release of mTHPP from bead is attributed to the polymer characteristics. In addition, diffusion of mTHPP may have been hindered by increased tortuosity of polymer accompanied by a swelling mechanism. Also, Saboktakin, *et al.* have been developed carboxymethyl starch (CMS) and dextran sulfate (DS) hydrogels that are able to efficiently encapsulate 5, 10, 15, 20-tetrakis(*meso*-hydroxyphenyl) porphyrin (mTHPP), a porphyrin-based PS agent. The study showed that the lifetime of the triplet state for porphyrin PS is significantly increase when encapsulate into hydrogel. In addition to the possible enhancement of  $^1O_2$  generation, other advan-

tages to incorporating porphyrin-based PS agents into hydrogel include the ability to solubilize these generally hydrophobic agents, the small and uniform size of hydrogels, and potential for passive targeting of solid tumors via the enhanced permeation and retention effect decreasing systemic photosensitization. This novel type of carboxymethyl starch (CMS) hydrogel using dextran sulfate (DS) as a polyanionic polymer was developed to achieve complex co-assembly for the incorporation and controlled release of an anti-angiogenesis hexapeptide, this was the first report describing the use of DS to formulate CMS based hydrogels. The mTHPP loaded CMS-DS hydrogels were characterized by FESEM for their size and distribution. Data showed that hydrogel have a solid and near consistent structure. These hydrogels have good spherical geometry. The results show that the surface of CMS-DS hydrogels shrank and a densely crosslinked gel structure was formed. The retardation of drug release from matrices of higher cross linker content. The average drug entrapment was found to be  $92.18 \pm 0.10$  % in the hydrogel. The size of CMS-DS hydrogels was estimated by scanning electron microscopy (SEM) of the dried hydrogel dispersions. The determination of hydrogel size by SEM under a dry state does not result in an accurate absolute value of the hydrated hydrogel size in dispersion, but only visualizes size range and particle shape. SEM analyses confirmed the relatively broad size distribution of the CMS-DS hydrogels, ranging from about 40-100 nm. The incorporation of mTHPP into the CMS-DS hydrogel produced a smooth surface and compact structure. The CMS-DS hydrogels are hydrophilic and would be expected to swell in water, thus producing a large hydrodynamic size when measured by the Zetasizer. The particle size of hydrogels is measured. Loading content of mTHPP hydrogels with different theoretical loading densities were analyzed. Drug loading density, loading efficiency, and mTHPP and hydrogel yields of the hydrogel with 5, 10, 20% theoretical loading densities were calculated. Results show that mTHPP was effectively loaded into CMS-DS hydrogels, with high loading efficiency in all formulations. mTHPP loading densities for 5, 10 and 20% theoretical loading were  $4.6 \pm 0.1$ ,  $9.8 \pm 0.2$ ,  $16.8 \pm 0.3$ %, respectively. Net loading efficiencies of 5, 10% theoretical loading were quantitative, whereas that of 20% theoretical loading was  $89.26 \pm 1.5$ %. The mTHPP and hydrogel yields were also sufficiently high to confirm hydrogel encapsulation of mTHPP as an effective strategy for solubilization of PS. The incorporation of mTHPP into the CMS-DS hydrogel resulted in a sharp increase in the particle size of the nanoparticle dispersion. mTHPP -loaded hydrogel was obtained spontaneously upon the mixing of the DS aqueous solution (0.1%, w/v) with the

CMS solution (0.1%, w/v) under magnetic stirring, with mTHPP dissolved in CMS-DS solution. The incorporation of mTHPP into the CMS-DS hydrogel resulted in a sharp increase in the particle size of the nanoparticle dispersion. The significant increases in particle size give a good induction of the incorporation of mTHPP into CMS-DS hydrogel. A study was undertaken to investigate the effect of the order of mTHPP mixing with CMS and DS. The data obtained show that the order of mTHPP mixing had no effect on the size, entrapment efficiency, and yield of mTHPP - loaded hydrogel. The loading efficiency and loading capacity of the nanoparticle dispersions are presented. It was shown that mTHPP/polymer feed ratios up to 20% (w/w), the loading efficiency was almost quantitative, resulting in loading capacities up to 20% and an mTHPP concentration in the dispersion of 1.3 mg/mL, which is markedly higher than the aqueous solubility of mTHPP. At 8% (w/w) loading, the dispersions stayed clear for more than a week. At higher loading of 15% and 20% (w/w), a precipitate was observed in the dispersions of loaded hydrogel within 1 days after preparation, indicating that the loading capacity of these hydrogels was exceeded. In contrast, the hydrogel composed of polymer remained clear for more than a week at 20% and 2 days for 30% loading, which demonstrates that these end groups have a favorable effect on the loading and solubilization capacity of the hydrogel. Mohammad Reza Saboktakin, *et al.* have been discussed some of the interesting findings and applications of modified chitosan (MCS) and their derivatives in different areas of drug delivery. This research highlights the important applications of MCS in the design of various novel delivery systems like liposomes, microspheres, microcapsules, and nanoparticles. In addition to their well-known effects on drug solubility and dissolution, bioavailability, safety, and stability, their uses as recipients in drug formulation are also discussed. This book also focuses on various factors influencing inclusion complex formation because an understanding of the same is necessary for proper handling of the versatile materials. Some important considerations in selecting MCS in drug formulation such as their commercial availability, regulatory status, and patent status are also summarized [2]. Photodynamic therapy (PDT) is a medical treatment in which a combination of a photosensitising drug and visible light causes destruction of selected cells. Over the past two decades, photodynamic therapy has enjoyed a period of intense investigation, both in the laboratory and in the clinic. Although still widely considered to be an experimental technique, its status and value within modern clinical practice continues to grow. The PDT field has, to date, been dominated by a small number of pharmaceutical

companies and inhabited almost exclusively by clinicians and those involved in fundamental scientific research. True pharmaceutical formulation development has been limited, to some extent, by financial constraints. If PDT is to realize its undoubted potential in clinical practice it is important for appropriate photosensitizer delivery system is raised. Accordingly, this article deals with the innovations pertaining to drug delivery systems for photodynamic therapy as disclosed in recent patent literature [3]. Nano delivery systems have shown considerable promise in increasing the solubility and delivery efficiency of hydrophobic photosensitizers for photodynamic therapy (PDT) applications. In this study, has been reported the preparation and characterization of polymeric micelles that incorporate protoporphyrin IX (PpIX), a potent photosensitizer, using non-covalent encapsulation and covalent conjugation methods. Depending on the incorporation method and PpIX loading percentage, PpIX existed as a monomer, dimer or aggregate in the micelle core.

The PpIX state directly affected the fluorescence intensity and  $^1\text{O}_2$  generation efficiency of the resulting micelles in aqueous solution. Micelles with lower PpIX loading density (e.g. 0.2%) showed brighter fluorescence and higher  $^1\text{O}_2$  yield than those with higher PpIX loading density (e.g. 4%) in solution. However, PDT efficacy in H2009 lung cancer cells showed an opposite trend. In particular, 4% PpIX-conjugated micelles demonstrated the largest PDT therapeutic window, as indicated by the highest phototoxicity and relatively low dark toxicity. Results from this study contribute to the fundamental understanding of nanoscopic structure–property relationships of micelle-delivered PpIX and establish a viable micelle formulation (i.e. 4%PpIX-conjugated micelles) for *in vivo* evaluation of antitumor efficacy [4]. Given the ever increasing problem of antibiotic resistance in nosocomial pathogens it is important to promote alternate technologies that may be more effective than current antibiotics. The Photodynamic Antimicrobial Chemotherapy (PACT), is a technology based on the use of a photosensitizer activated by visible light illumination and found to be effective against most types of microbial pathogens, including those resistant to antibiotics. PACT nonetheless has certain limitations, particularly against internal and blood-borne infections. To this end, we are developing Chemiluminescent Photodynamic Antimicrobial Therapy (CPAT). The practical advantages of CPAT emphasize that this novel technique could expand efforts to control nosocomial pathogens, including those responsible for systemic infections [5]. Photodynamic therapy (PDT) is an emerging the ranostic modal-

ity for various cancer as well as non-cancer diseases. Its efficiency is mainly based on a selective accumulation of PDT and imaging agents in tumor tissue. The vascular effect is widely accepted to play a major role in tumor eradication by PDT. To promote this vascular effect, we previously demonstrated the interest of using an active- targeting strategy targeting neuropilin-1 (NRP-1), mainly over-expressed by tumor angiogenic vessels. For an integrated vascular-targeted PDT with magnetic resonance imaging (MRI) of cancer, we developed multifunctional gadolinium-based nanoparticles consisting of a surface-localized tumor vasculature targeting NRP-1 peptide and polysiloxane nanoparticles with gadolinium chelated by DOTA derivatives on the surface and a chlorin as photosensitizer. The nanoparticles were surface-functionalized with hydrophilic DOTA chelates and also used as a scaffold for the targeting peptide grafting. *In vitro* investigations demonstrated the ability of multifunctional nanoparticles to preserve the photophysical properties of the encapsulated photosensitizer and to confer photosensitivity to MDA-MB-231 cancer cells related to photosensitizer concentration and light dose. Using binding test, we revealed the ability of peptide-functionalized nanoparticles to target NRP-1 recombinant protein. Importantly, after intravenous injection of the multifunctional nanoparticles in rats bearing intracranial U87 glioblastoma, a positive MRI contrast enhancement was specifically observed in tumor tissue. Real-time MRI analysis revealed the ability of the targeting peptide to confer specific intratumoral retention of the multifunctional nanoparticles [6]. In this research has been addressed a highly interdisciplinary field, the use of nanomaterials as carriers for singlet oxygen photosensitizers and their potential applications in photodynamic therapy. In particular, recent advances in the use of nanoparticles including inorganic oxide, metallic-, and polymer-based nanocomposites as photo sensitizer carriers are highlighted. The advantages and shortcomings of these diverse has been approach as far as their application for photodynamic therapy is concerned. Fullerenes and their derivatives are also included, focusing on recent studies on their structure, properties, and ability to generate singlet oxygen [7]. The Photodynamic therapy (PDT) is a promising treatment modality for cancer. PDT is based on the concept that photosensitizers, when exposed to light of specific wavelength, generate cytotoxic reactive oxygen species (ROS) capable of killing tumor cells. The effectiveness of PDT has been limited in part by the lack of photosensitizers that accumulate sufficiently in tumor cells and poor yield of ROS from existing photosensitizers. In this report has been investigated whether aerosol OT-alginate



nanoparticles can be used as a carrier to enhance the therapeutic efficacy of a model photosensitizer, methylene blue. Methylene blue loaded nanoparticles were evaluated for PDT effectiveness in two cancer cell lines, MCF-7 and 4T1. Encapsulation of methylene blue in nanoparticles significantly enhanced intracellular ROS production, and the overall cytotoxicity following PDT. It also resulted in higher incidence of necrosis. Greater effectiveness of nanoparticles could be correlated with higher yield of ROS with nanoparticle-encapsulated methylene blue. Further, treatment of tumor cells with nanoparticle-encapsulated methylene blue resulted in significant nuclear localization of methylene blue while free drug treatment resulted in its accumulation mainly in the endolysosomal vesicles. In conclusion, encapsulation of methylene blue in aerosol OT-alginate nanoparticles enhanced its anticancer photodynamic efficacy *in vitro*. Increased ROS production and favorable alteration in the subcellular distribution contribute to the enhanced PDT efficacy of nanoparticle-encapsulated photosensitizer [8].

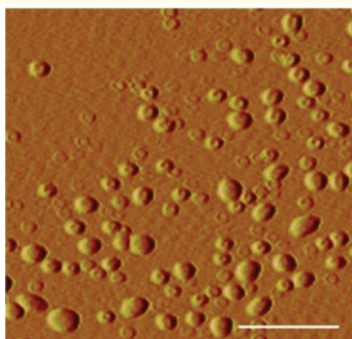


**Figure 1:** AFM image of methylene blue-loaded nanoparticles in the tapping mode in air. The image is an amplitude image of a representative sample spot. Length of the bar is 500 nm.

A novel process for the production of three-layer Composite Nanoparticles (CNPs) in the size range 100-300 nm has been reported with an upconverting phosphor interior; a coating of porphyrin photosensitizer, and a biocompatible PEG outer layer to prevent clearance by the reticuloendothelial system. This report shows that these CNPs produce millimolar amounts of singlet oxygen at NIR intensities far less than other two-photon techniques [9]. Photodynamic therapy (PDT) is an emerging clinical modality for the treatment of a variety of diseases. Most photosensitizers are hydrophobic and poorly soluble in water. Many new nanoplate forms have

been successfully established to improve the delivery efficiency of PS drugs. However, few reported studies have investigated how the carrier micro environment may affect the photophysical properties of photosensitizer (PS) drugs and subsequently, their biological efficacy in killing malignant cells. In this study, has been described the modulation of type I and II photo activation processes of the photosensitizer, 5, 10, 15, 20-tetrakis(meso-hydroxyphenyl)porphyrin (mTHPP), by the micelle core environment. Electron-rich poly(2-

(diisopropylamino)ethyl methacrylate) (PDPA) micelles increased photoactivations from type II to type I mechanisms, which significantly increased the generation of  $O_2^{\cdot -}$  through the electron transfer pathway over  $^1O_2$  production through energy transfer process. The PDPA micelles led to enhanced phototoxicity over the electron-deficient poly(D,L-lactide) control in multiple cancer cell lines under argon-saturated conditions. These data suggest that micelle carriers may not only improve the bioavailability of photosensitizer drugs, but also modulate photophysical properties for improved PDT efficacy [10]. Nano delivery systems have shown considerable promise in increasing the solubility and delivery efficiency of hydrophobic photosensitizers for photodynamic therapy (PDT) applications. In this study, has been reported the preparation and characterization of polymeric micelles that incorporate protoporphyrin IX (PpIX), a potent photosensitizer, using non-covalent encapsulation and covalent conjugation methods. Depending on the incorporation method and PpIX loading percentage, PpIX existed as a monomer, dimer or aggregate in the micelle core. The PpIX state directly affected the fluorescence intensity and  $^1O_2$  generation efficiency of the resulting micelles in aqueous solution. Micelles with lower PpIX loading density (e.g. 0.2%) showed brighter fluorescence and higher  $^1O_2$  yield than those with higher PpIX loading density (e.g. 4%) in solution. However, PDT efficacy in H2009 lung cancer cells showed an opposite trend. In particular, 4% PpIX conjugated micelles demonstrated the largest PDT therapeutic window, as indicated by the highest phototoxicity and relatively low dark toxicity. Results from this study contribute to the fundamental understanding of nanoscopic structure–property relationships of micelle-delivered PpIX and establish a viable micelle formulation (i.e. 4% PpIX-conjugated micelles) for *in vivo* evaluation of antitumor efficacy [11]. A new study describe to develop carboxymethyl starch(CMS) and dextran sulfate (DS) hydrogels that are able to efficiently encapsulate 5, 10, 15, 20-tetrakis(meso-hydroxyphenyl) porphyrin (mTHPP), a porphyrin-based PS agent.

The study showed that the lifetime of the triplet state for porphyrin PS is significantly increase when encapsulate into hydrogel. In addition to the possible enhancement of  $^1O_2$  generation, other advantages to incorporating porphyrin-based PS agents into hydrogel include the ability to solubilize these generally hydrophobic agents, the small and uniform size of hydrogels, and potential for passive targeting of solid tumors via the enhanced permeation and retention effect decreasing systemic photosensitization. This novel type of carboxymethyl starch (CMS) hydrogel using dextran sulfate (DS) as a polyanionic polymer was developed to achieve complex coacervation for the incorporation and controlled release of an anti-angiogenesis hexapeptide, this was the first report describing the use of DS to formulate CMS based hydrogels [12]. The development of new nanoscale drug carriers, chitosan-based nanoparticles (CNPs) shows that can be used for photodynamic therapy. These carriers could encapsulate a photosensitizer, protoporphyrin IX (PpIX), and deliver it to tumor tissue. It has been reported that CNPs presented the enhanced tumor target specificity in cancer therapy and imbibed various water insoluble anticancer agents into the hydrophobic multicores of nanoscale particles. In this study, has been prepared photosensitizer- encapsulated CNPs by self-assembling amphiphilic glycol chitosan-5b-cholanic acid conjugates in an aqueous environment and then encapsulating the water-insoluble photosensitizer (PpIX), with high drug-loading efficiency (>90%) by using a dialysis method. Freshly prepared PpIX-encapsulated CNPs (PpIX-CNPs) had an average diameter of 290 nm and were stable in aqueous solutions for 1 month. As nanoscale drug carriers, PpIX-CNPs exhibited a sustained release profile *in vitro* and were non-toxic to tumor cells in the dark. In a cell culture system, has been observed rapid cellular uptake of the PpIX-CNPs and the released PpIX from CNPs became highly phototoxic upon visible irradiation. In SCC7 tumor-bearing mice, PpIX-CNPs exhibited enhanced tumor specificity and increased therapeutic efficacy compared to free PpIX. Taken together, these results indicate that PpIX-CNPs have potential as an effective drug delivery system for clinical photodynamic therapy [14]. Pancreatic cancer (PanCa) has a poor prognosis with a 5-year survival rate of only 5%. Photodynamic therapy (PDT) has shown promising results in treating PanCa. Mechanism-based combinations with PDT have enhanced treatment outcome. Agents tested with PDT include Avastin, an antibody against vascular endothelial growth factor (VEGF) which is approved for treating various cancers. Simultaneous delivery of drugs in nano-constructs could improve the treatment response of

mechanism based combination therapies. Here, has been investigated the effect of neutralizing VEGF using nanotechnology for the delivery of Avastin in combination with PDT. For this has been used a construct called “nanocells” in which the photosensitizer was trapped inside polymer nanoparticles and these, with Avastin, were then encapsulated inside liposomes. *In vitro*, nano cells containing Avastin (NCA) significantly enhanced cytotoxicity in PanCa cells. NCA based PDT also significantly improved treatment response in mice that were orthotopically implanted with PanCa. Avastin delivered extra cellularly in combination with PDT did not show any improvement. Here a new paradigm for Avastin-based therapy by combining intracellular delivery of the antibody and PDT using nanotechnology has been showed for treating PanCa [15]. Although photodynamic therapy is considered as a noninvasive method, most photosensitizers are susceptible to ultrasound. Therefore, it is expected that the combination of two activation methods might have a synergistic effect. This probable effect has been investigated in this study. This study was conducted on colon carcinoma tumor in Balb/c mice. The tumors were induced by subcutaneous injection of CT26 cells. Ultrasound and light irradiations were performed on tumors 24 hr after injection of liposomal Zn (II)-phthalocyanine. The treatment efficacy was evaluated using daily measurement of the tumor dimensions. Ten days post treatment, relative tumor volumes of all groups were significantly reduced in comparison with the main control group. The best response was observed when one of the two treatment methods had been applied. The longest doubling time of tumor was related to the treatment group namely photodynamic, sonodynamic and combination technique, while the shortest belonged to the control group. This study showed that liposomal Zn phthalocyanine is both photosensitizer and sonosensitizer. Photodynamic and sonodynamic therapies can be efficient in retarding tumor growth rate. In this study, the combination of two methods didn't show any improvement in therapeutic outcomes. It is predicted that latest results are related to the treatments sequence and could be optimized in the future [16]. A novel post-loading approach for constructing a multifunctional biodegradable polyacrylamide (PAA) nanoplatform has been reported for tumorimaging (fluorescence) and photodynamic therapy (PDT). This approach provides an opportunity to post-load the imaging and therapeutic agents at desired concentrations. Among the PAA nanoparticles, a formulation containing the photosensitizer, HPPH [3-(1'-hexyloxyethyl) pyropheophorbide-a], and the cyanine dye in a ratio of 2:1 mini-

mized the undesirable quenching of the HPPH electronic excitation energy because of energy migration within the nanoparticles and/or Förster (fluorescence) resonance energy transfer (FRET) between HPPH and cyanine dye. An excellent tumor-imaging (NIR fluorescence) and phototherapeutic efficacy of the nano construct formulation is demonstrated. Under similar treatment parameters the HPPH in 1% Tween 80/5% aqueous dextrose formulation was less effective than the nano construct containing HPPH and cyanine dye in a ratio of 2 to 1. This is the first example showing the use of the post loading approach in developing a nano constructs for tumor-imaging and therapy [17]. Nanoparticles can be targeted towards, and accumulate in, tumor tissue by the enhanced permeability and retention effect, if sequestration by the reticuloendothelial system (RES) is avoided. The application of nanoparticles in the field of drug delivery is thus an area of great interest, due to their potential for delivering high payloads of drugs site selectively. One area which may prove to be particularly attractive is photodynamic therapy, as the reactive oxygen species (ROS) which cause damage to the tumor tissue are not generated until the drug is activated with light, minimizing generalized toxicity and giving a high degree of spatial control over the clinical effect. In the present study, has been synthesized two types of nanoparticles loaded with photodynamic sensitizers: polylysine bound tetrasulfonato-aluminum phthalocyanine entrapped nanoparticles (PCNP) and polylysine bound tetrasulfonato-aluminum phthalocyanine entrapped nanoparticles coated with a second, porphyrin based, photosensitizer (PCNP-P) to enhance the capacity for ROS generation, and hence therapeutic potential. The mean sizes of these particles were 45 (10 nm) and 95 (10 nm) respectively. Uptake of the nanoparticles by human Caucasian colon adenocarcinoma cells (HT29) was determined by flow cytometry and confocal microscopy. Cell viability assays using PCNP-P and PCNP corresponding to the minimum uptake time (<5 min) and maximum uptake time (25 h) demonstrated that these cancer cells can be damaged by light activation of these photodynamic nanoparticles both in the external media and after internalization. The results suggest that, in order to induce photodynamic damage, the nanoparticles need only to be associated with the tumor cell closely enough to deliver singlet oxygen: their internalization within target cells may not be necessary. Clinically, this could be of great importance as it may help to combat the known ability of many cancer cells to actively expel conventional anticancer drugs [18]. The rationales for the use of water soluble polymers for anticancer drug delivery include: the potential to overcome some forms of multidrug resistance,

preferential accumulation in solid tumors due to enhanced permeability and retention (EPR) effect, biorecognition ability, and target ability. The utility of a novel paradigm for the treatment of ovarian carcinoma in an experimental animal model, which combines chemotherapy and photodynamic therapy with polymer-bound anticancer drugs is explained. Research and clinical applications as well as directions for the future development of macromolecular therapeutics are discussed [19]. The study of singlet molecular oxygen production and reactivity has emerged as a rich and diverse area with implications in fields ranging from polymer science to cancer therapy. In this study, has been addressed the photophysical properties of singlet oxygen and of the photosensitizers used in its generation. Photosensitizers based on organic molecules and coordination compounds are examined and compared. Recent advances in the photosensitized production of singlet oxygen and its uses in photochemistry and photobiology are highlighted, with particular focus on its role in wastewater treatment, fine chemical synthesis, and photodynamic therapy (PDT). Future directions in photosensitizer development and singlet oxygen applications are also explored [20]. Herein, has been developed the photosensitizer, protoporphyrin IX (PpIX), conjugated glycol chitosan (GC) nanoparticles (PpIXeGCeNPs) as tumor-homing drug carriers with cellular on/off system for photodynamic imaging and therapy, simultaneously. In order to prepare PpIXeGCeNPs, hydrophobic PpIXs were chemically conjugated to GC polymer and the amphiphilic PpIXeGC conjugates formed a stable nanoparticle structure in aqueous condition, wherein conjugated PpIX molecules formed hydrophobic innercores and they were covered by the hydrophilic GC polymer shell. Based on the nanoparticle structure, PpIXeGCeNPs showed the self-quenching effect that is 'off' state with no fluorescence signal and phototoxicity with light exposure. It is due to the compact crystallized PpIX molecules in the nanoparticles as confirmed by dynamic light scattering and X-ray diffraction methods. However, after cellular uptake, compact nanoparticle structure gradually decreased to generate strong fluorescence signal and singlet oxygen generation when irradiated. Importantly, PpIXeGCeNPs-treated mice presented prolonged blood circulation, enhanced tumor targeting ability, and improved *in vivo* therapeutic efficiency in tumor-bearing mice, compared to that of free PpIX treated mice. These results proved that this tumor homing cellular 'on/off' nanoparticle system of PpIXeGCeNPs has a great potential for synchronous photodynamic imaging and therapy in cancer treatment [21]. A method based on mass spectrometry has been reported for the characterization of noncovalent complexes of proteins with

mixtures of ligands; this method is relevant to the study of drug leads and may be useful in screening libraries for tight-binding compounds. It is based on the ability of electrospray ionization (ESI)'s2 to generate ions of intact noncovalent complexes in the gas phase and of Fourier transform ion cyclotron resonance (FTICR) mass spectrometry to perform dz-selective ion accumulation, I0 isolation, and multistage ion dissociation to obtain structural information about these complexes (including the identification of the structure of the bound ligand). Here, has been described a study of the competitive binding of inhibitors derived from para-substituted benzene sulfonamides to bovine carbonic anhydrase I1 (BCAII, EC 4.2.1.1) using this technique. Relative binding constants and structural information for a mixture of inhibitors can be obtained in a single experiment using ESI-FTICR-MS [22]. Treatment of brain cancer remains a challenge despite recent improvements in surgery and multimodal adjuvant therapy. Drug therapies of brain cancer have been particularly inefficient, due to the blood-brain barrier and the non-specificity of the potentially toxic drugs. The nanoparticle has emerged as a potential vector for brain delivery, able to overcome the problems of current strategies. Moreover, multi-functionality can be engineered into a single nanoplatform so that it can provide tumor specific detection, treatment, and follow-up monitoring. Such multi tasking is not possible with conventional technologies. This research describes recent advances in nanoparticle-based detection and therapy of brain cancer. The advantages of nanoparticle based delivery and the types of nanoparticle systems under investigation are described, as well as their applications [23]. The development of photosensitizer-conjugated gold nanorods (MMP2P-GNR) has been described in which photosensitizers were conjugated onto the surface of gold nanorods (GNR) via a protease-cleavable peptide linker. It has been hypothesized that fluorescence and phototoxicity of the conjugated photosensitizers would be suppressed in their native state, becoming activated only after cleavage by the target protease matrix metalloprotease-2 (MMP2). Quantitative analysis of the fluorescence and singlet oxygen generation (SOG) demonstrated that the MMP2P-GNR conjugate emitted fluorescence intensity corresponding to 0.4% ~ 0.01% and an SOG efficiency of 0.89% ~ 1.04% compared to free pyropheophorbide-a. From the *in vitro* cell studies using HT1080 cells that overexpress MMP2 and BT20 cells that lack MMP2, we observed that fluorescence and SOG was mediated by the presence or absence of MMP2 in these cell lines. This novel activatable photosensitizing system may be useful for protease-mediated fluorescence imaging and subsequent photodynamic therapy

for various cancers [24]. Intense research has led to a more comprehensive understanding of cancer at the genetic, molecular, and cellular levels providing an avenue for methods of increasing anti-tumor efficacy of drugs while reducing systemic side effects. Nanoparticulate technology is of particular use in developing a new generation of more effective cancer therapies capable of overcoming the many biological, biophysical, and biomedical barriers that the body stages against a standard intervention. Nanoparticles show much promise in cancer therapy by selectively gaining access to tumor due to their small size and modifiability. Typically, though not exclusively, nanoparticles are defined as sub microscopic particles between 1 and 100 nm. Nanoparticles are formulated out of a variety of substances and engineered to carry an array of substances in a controlled and targeted manner. Nanoparticles are prepared to take advantage of fundamental cancer morphology and modes of development such as rapid proliferation of cells, antigen expression, and leaky tumor vasculature. In cancer treatment and detection nanoparticles serve many targeted functions in chemotherapy, radiotherapy, immunotherapy, immunodetection, thermotherapy, imaging, photodynamic therapy, and anti-angiogenesis. Not only are modifying agents allowing for greater and more accurate tumor targeting, they are also aiding in the crossing of biophysical barriers such as the blood brain barrier there by reducing peripheral effects and increasing the relative amount of drug reaching in the brain. Moreover, multifunctional nanoparticles perform many of these tasks simultaneously such as targeted delivery of a potent anticancer drug at the same time as an imaging material to visualize the effectiveness of the drug utilized for treatment follow-up. In this book, several recent US and World patents developing and modifying nanoparticles for the detection, analysis, and treatment of cancer are discussed [25]. The utility of chitosan nanoparticles has been evaluated with an invitro model of acrolein-mediated cell injury using PC -12 cells. The particles effectively, and statistically, reduced damage to membrane integrity, secondary oxidative stress, and lipid peroxidation. This study suggests that a chitosan nanoparticle-based therapy to interfere with "secondary" injury may be possible. Hydralazine-loaded chitosan nanoparticles were prepared using different types of polyanions and characterized for particle size, morphology, zeta potential value, and the efficiency of hydralazine entrapment and release. Hydralazine-loaded chitosan nanoparticles ranged in size from 300 nm to 350 nm in diameter, and with a tunable, or adjustable, surface charge [26]. A novel research have been developed superparamagnetic chitosan(CS) – dextran sulfate(DS) hydrogels as a intelli-



gent drug system for effective carrying of Chlorin E6 photosensitizer to cancer cells. This system can be detectable by magnetic Resonance Imaging technique. The study shows that the lifetime of the triplet state for chn E6 photosensitizer is significantly increase when encapsulate into hydrogel. In addition to the possible enhancement of  $^1O_2$  generation, other advantages to incorporating chlorin E6 based PS agents into hydrogel include the ability to solubilize these generally hydrophobic agents, the small and uniform size of hydrogels, and potential for passive targeting of solid tumors *via* the enhanced permeation and retention effect decreasing systemic photosensitization. The chlorin E6 loaded CS-DS hydrogels were characterized by FESEM for their size and distribution. Data showed that hydrogel have a solid and near consistent structure [27-40]. These hydrogels have good spherical geometry. Figure 2 shows a representative SEM image of chlorin E6 hydrogels. Also, the results show that the surface of CS-DS hydrogels shrank and a densely cross-linked gel structure was formed. The retardation of drug release from matrices of higher cross linker content. The average drug entrapment was found to be  $92.18 \pm 0.10$  % in the hydrogel. The size of CS-DS hydrogels was estimated by scanning electron microscopy(SEM) of the dried hydrogel dispersions. The determination of hydrogel size by SEM under a dry state does not result in an accurate absolute value of the hydrated hydrogel size in dispersion, but only visualizes size range and particle shape.. SEM analyses confirmed the relatively broad size distribution of the CS-DS hydrogels, ranging from about 40100 nm. The incorporation of chlorin E6 into the CS-DS hydrogel produced a smooth surface and compact structure. The CS-DS hydrogels are hydrophilic and would be expected to swell in water, thus producing a large hydrodynamic size when measured by the Zetasizer.

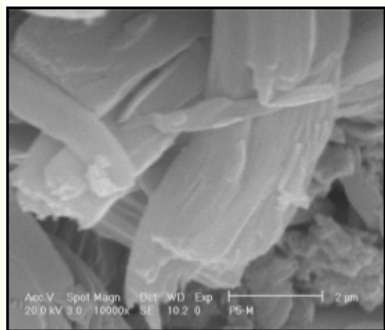


**Figure 2:** Morphology of ch E6 loaded CS-DS hydrogel by emission scanning electron microscopy field.

The incorporation of chlorin E6 into the CS-DS hydrogel resulted in a sharp increase in the particle size of the nanoparticle dispersion. Chlorin E6 -loaded hydrogel was obtained spontaneously upon the mixing of the DS aqueous solution (0.1%, w/v) with the CS solution (0.1%, w/v) under magnetic stirring, with chn E6 dissolved in CS-DS solution. The incorporation of Chlorin E6 into the CS- DS hydrogel resulted in a sharp increase in the particle size of the nanoparticle dispersion. The significant increases in particle size give a good induction of the incorporation of Chlorin E6 into CS-DS hydrogel. A study was undertaken to investigate the effect of the order of Chlorin E6 mixing with CS and DS. The data obtained show that the order of Chlorin E6 mixing had no effect on the size, entrapment efficiency, and yield of chn E6 -loaded hydrogel. The loading efficiency and loading capacity of the nanoparticle dispersions are presented in Figure 3a and 3b, respectively. It was shown that Chlorin E6/polymer feed ratios up to 30%(w/w), the loading efficiency was almost quantitative, resulting in loading capacities up to 30% and an Chlorin E6 concentration in the dispersion of 1.8 mg/mL, which is markedly higher than the aqueous solubility of Chlorin E6. At 10% (w/w) loading, the dispersions stayed clear for more than a week. At higher loading of 20% and 30% (w/w), a precipitate was observed in the dispersions of loaded hydrogel within 1 days after preparation, indicating that the loading capacity of these hydrogels was exceeded. In contrast, the hydrogel composed of polymer remained clear for more than a week at 20% and 2 days for 30% loading, which demonstrates that these end groups have a favorable effect on the loading and solubilization capacity of the hydrogel.

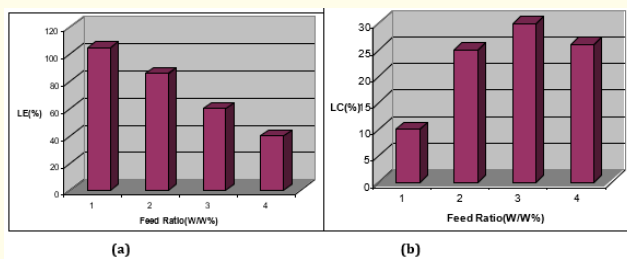


**Figure 3:** (a) Loading efficiency and (b) loading capacity of CS-DS hydrogel with chlorin E6.

The *in vitro* photocytotoxicity effect of Chlorin E6 loaded hydrogel on  $^{14}C$  cells was determined after 6 h incubation and compared with free chlorin E6. Either various dilutions of loaded nanoparti-

cles at a fixed Chlorin E6/polymer ratio of 15%(w/w) were used, or the polymer concentration was fixed at 0.5 mg/mL and the chlorin E6 loading was varied between 0.004% and 0.32%(w/w) in order to secure a polymer concentration of ~100 times above its critical aggregation concentration. The results demonstrate that the effect on the viability of  $^{14}\text{C}$  cells of chlorin E6 – polymer hydrogel at a fixed chlorin E6/polymer ratio is comparable to that of free chlorin E6. At a fixed high polymer concentration, the nanoparticles with various loadings were hardly toxic to cells even at the highest chlorin E6 concentration used, as indicated by a cell viability of 80%. Loaded hydrogel, and free Chlorin E6 were diluted in medium to a concentration of 12  $\mu\text{M}$  and incubated with  $^{14}\text{C}$  cells for 6 h to determine the cellular uptake of chlorin E6. The 15% (w/w) chlorin loaded and polymer nanoparticles showed a lower cellular uptake of chlorin E6 compared to free chlorin E6, by a factor of 2.8 and 3.7, respectively. More importantly, hardly any chlorin E6 uptake was measured after incubation with the hydrogel yielding a cellular uptake comparable of free chlorin E6. The results of the photocytotoxicity and cellular uptake of the different formulations suggest that when the concentration of polymer is kept well above, chlorin E6 remains stably encapsulated in the hydrogel even in the presence of serum, and that the intact nanoparticles are not taken up by the cells, which may be ascribed to the presence of a dense polymer-layer. Only after dilution of the chlorin E6 -loaded hydrogel to polymer concentrations below and after hydrogel degradation, the released chlorin E6 can be taken up by  $^{14}\text{C}$  cells and exert its cytotoxic effect upon illumination. Nano polymer bonded Chlorin E6 (50 mg) were poured into 3 mL of aqueous buffer solution (pH 7.4) (Figure 4).

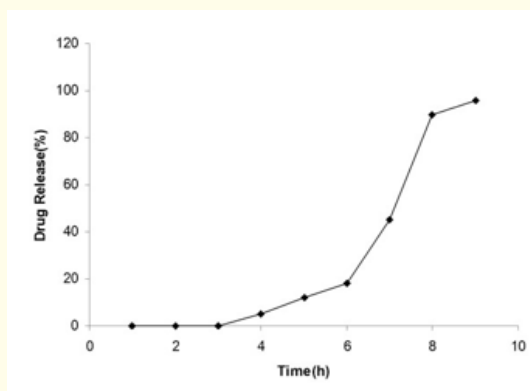


**Figure 4:** Release of chlorin E6 from CS-DS hydrogel at 37°C.

The mixture was introduced into a cellophane membrane dialysis bag. The bag was closed and transferred to a flask containing 20 mL of the same solution maintained at 37° C. The external solution was continuously stirred, and 3 mL samples were removed at selected intervals. The triplicate samples were analyzed by UV spectrophotometer, and the quantity of Chlorin E6 were determined using a standard calibration curve obtained under the same conditions. The primary mechanism for release of chlorin E6 from matrix systems *in vitro* are swelling, diffusion, and disintegration. *In vitro* degradation of CS-DS hydrogels were prepared by solution casting method occurred less rapidly as the degree 73% deacetylated showed slower biodegradation. Since the grade of CS-DS used in the present study was of high molecular weight with a degree of deacetylation  $\geq 85\%$ , significant retardation of release of chlorin E6 from bead is attributed to the polymer characteristics. In addition, diffusion of chlorin E6 may have been hindered by increased tortuosity of polymer accompanied by a swelling mechanism (Figure 5).

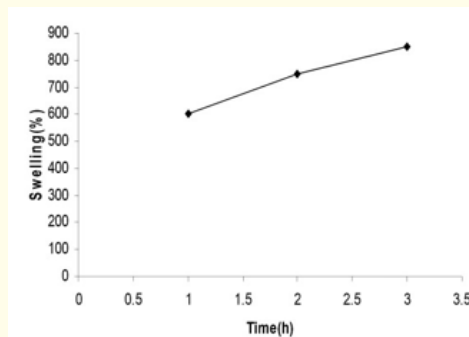


**Figure 5:** Time-dependent swelling behavior of chlorin E6 loaded CS-DS hydrogel at 37°C.

## Conclusion

Nano delivery systems have shown considerable promise in increasing the solubility and delivery efficiency of hydrophobic photosensitizers for photodynamic therapy (PDT) applications.

## Bibliography

1. Mohammad Reza Saboktakina., *et al.* "Synthesis and *in vitro* studies of biodegradable modified chitosan nanoparticles for photodynamic treatment of cancer". *International Journal of Biological Macromolecules* 49 (2011) 1059-1065.

2. Mohammad Reza Saboktakin., *et al.* "Intelligent Drug Delivery Systems Based on Modified Chitosan Nanoparticles". *Letters in Organic Chemistry* 9 (2012): 56-70.
3. Ryan F Donnelly., *et al.* "Drug Delivery Systems for Photodynamic Therapy". *Recent Patents on Drug Delivery and Formulation* 3 (2009): 1-7.
4. Huiying Ding., *et al.* "Nanoscope micelle delivery improves the photophysical properties and efficacy of photodynamic therapy of protoporphyrin IX". *Journal of Controlled Release* 151 (2011): 271-277.
5. Faina Nakonechny., *et al.* "New techniques in antimicrobial photodynamic therapy: scope of application and overcoming drug resistance in nosocomial infections". *Science against microbial pathogens: communicating current research and technological advances Méndez-Vilas (Ed.)* (2011).
6. Hamanou Benachour., *et al.* "Multifunctional Peptide-Conjugated Hybrid Silica Nanoparticles for Photodynamic Therapy and MRI". *Theranostics* 2.9 (2012): 889-904.
7. Shizhong Wang., *et al.* "Nanomaterials and singlet oxygen photosensitizers: potential applications in photodynamic therapy". *Journal of Materials Chemistry* 14 (2004): 487-493.
8. Ayman Khdaif., *et al.* "Surfactant-Polymer Nanoparticles Enhance the Effectiveness of Anticancer Photodynamic Therapy". *Molecular Pharmaceutics* 5.5 (2008): 807.
9. Baris Ungun., *et al.* "Nanofabricated upconversion nanoparticles for photodynamic therapy". *Optics Express* 17.1 (2009): 80.
10. Huiying Ding., *et al.* "Photoactivation switch from type II to type I reactions by electron-rich micelles for improved photodynamic therapy of cancer cells under hypoxia". *Journal of Controlled Release* 156.3 (2011): 276-280.
11. Huiying Ding., *et al.* "Nanoscope micelle delivery improves the photophysical properties and efficacy of photodynamic therapy of protoporphyrin IX". *Journal of Controlled Release* 151 (2011): 271-277.
12. Mohammad Reza Saboktakina., *et al.* "Synthesis and Characterization of Modified Starch Hydrogels for Photodynamic Treatment of Cancer". *International Journal of Biological Macromolecules* 51 (2012): 544-549.
13. João Paulo Figueiró Longo., *et al.* "Nanostructured Carriers for Photodynamic Therapy Applications in microbiology". *Science against microbial pathogens: communicating current research and technological advances Méndez-Vilas (Ed.)*.
14. So Jin Lee., *et al.* "Tumor specificity and therapeutic efficacy of photosensitizer-encapsulated glycol chitosan-based nanoparticles in tumor-bearing mice". *Biomaterials* 30 (2009): 2929-2939.
15. Prakash Rai., *et al.* "Nanotechnology-based combination therapy improves treatment response in cancer models". *Proc. of SPIE* (2009).
16. Maryam Bakhshizadeh., *et al.* "Effects of Combined Sonodynamic and Photodynamic Therapies on a Colon Carcinoma Tumor Model". *Iranian Journal of Basic Medical Sciences* 14.3 (2011).
17. Anurag Gupta., *et al.* "Multifunctional nanoplatfoms for fluorescence imaging and photodynamic therapy developed by post-loading photosensitizer and fluorophore to polyacrylamide nanoparticles". *Nanomedicine: Nanotechnology, Biology, and Medicine* 8 (2012): 941-950.
18. Maheshika Kurupparachchi., *et al.* "Polyacrylamide Nanoparticles as a Delivery System in Photodynamic Therapy". *Molecular Pharmaceutics* 8.3 (2011): 920-931.
19. J Kopec̣eka., *et al.* "Water soluble polymers in tumor targeted delivery". *Journal of Controlled Release* 74 (2001): 147-158.
20. Maria C., *et al.* "Photosensitized singlet oxygen and its applications". *Coordination Chemistry Reviews* 233/234 (2002): 351-371.
21. So Jin Lee., *et al.* "Tumor-homing photosensitizer-conjugated glycol chitosan nanoparticles for synchronous photodynamic imaging and therapy based on cellular on/off system". *Biomaterials* 32 (2011): 4021e4029.
22. Xueheng Cheng., *et al.* "Using Electrospray Ionization FTICR Mass Spectrometry To Study Competitive Binding of Inhibitors to Carbonic Anhydrase". *Journal of the American Chemical Society* 117 (1995): 8859-8860.
23. Yong-Eun Lee., *et al.* "Brain cancer diagnosis and therapy with nanoplatfoms". *Advanced Drug Delivery Reviews* 58 (2006): 1556-1577.
24. Niraj B Patel. "Targeted methylene blue-containing polymeric nanoparticle formulations for oral antimicrobial photodynamic therapy". (2009).
25. Boseung Jang and Yongdoo Choi. "Photosensitizer-Conjugated Gold Nanorods for Enzyme-Activatable Fluorescence Imaging and Photodynamic Therapy". *Theranostics* 2.2 (2012): 190-197.

26. Youngnam Cho., *et al.* "Chitosan nanoparticle based neuronal membrane sealing and neuroprotection following acrolein induced cell injury". *Journal of Biological Engineering* 4 (2010): 2.
27. Wagner V., *et al.* "The emerging nanomedicine landscape". *Nature Biotechnology* 24.10 (2006): 1211-1218.
28. Kim BY., *et al.* "Nanomedicine". *The New England Journal of Medicine* 363.25 (2010): 2434-2443 (2010).
29. Jacobson GB., *et al.* "Biodegradable nanoparticles with sustained release of functional siRNA in skin". *Journal of Pharmaceutical Sciences* 99.10 (2010): 4261-4266.
30. O'Brien ME., *et al.* "Reduced cardiotoxicity and comparable efficacy in a Phase III trial of pegylated liposomal doxorubicin HCl (CAELYX/doxil) versus conventional doxorubicin for first-line treatment of metastatic breast cancer". *Annals of Oncology* 15.3 (2004): 440-449.
31. Davis ME., *et al.* "Evidence of RNAi in humans from systemically administered siRNA via targeted nanoparticles". *Nature* 464.7291 (2010): 1067-1070.
32. Scranton R and Cincotta A. "Bromocriptine - unique formulation of a dopamine agonist for the treatment of Type 2 diabetes". *Expert Opinion on Pharmacotherapy* 11.2 (2010): 269-279.
33. Lim WT., *et al.* "Phase I pharmacokinetic study of a weekly liposomal paclitaxel formulation (Genexol-PM) in patients with solid tumors". *Annals of Oncology* 21.2 (2009): 382-388.
34. Winter PM., *et al.* "Molecular imaging of angiogenesis in early-stage atherosclerosis with avb3-integrin-targeted nanoparticles". *Circulation* 108.18 (2003): 2270-2274.
35. Keren S., *et al.* "Noninvasive molecular imaging of small living subjects using Raman spectroscopy". *Proceedings of the National Academy of Sciences of the United States of America* 105.15 (2008): 5844-5849.
36. Jain PK., *et al.* "Noble metals on the nanoscale: optical and photothermal properties and some applications in imaging, sensing, biology, and medicine". *Accounts of Chemical Research* 41.12 (2008): 1578-1586.
37. Maeda H., *et al.* "Tumor vascular permeability and the EPR effect in macromolecular therapeutics: a review". *Journal of Control Release* 65.1-2 (2000): 271-284.
38. Knop K., *et al.* "Poly (ethylene glycol) in drug delivery: pros and cons as well as potential alternatives". *Angewandte Chemie* 49.36 (2006): 6288-6308.
39. van Vlerken LE., *et al.* "Poly (ethylene glycol)-modified nanocarriers for tumor-targeted and intracellular delivery". *Pharmaceutical Research* 24.8 (2007): 1405-1414.
40. Kanaras AG., *et al.* "Thioalkylated tetraethylene glycol: a new ligand for water soluble monolayer protected gold clusters". *Chemical Communication* 20 (2002): 2294-2295.

**Volume 3 Issue 6 May 2021**

**© All rights are reserved by Mohammadreza Saboktakin.**